JOURNAL OF RADIOGRAPHY AND
RADIATION SCIENCES

PHOTON AND NEUTRON SHIELDING COMPETENCE OF SnO_2 – REINFORCED WITH $22Na_2O$ – $15B_2O_3$ – $45P_2O_5$ – (18 - x) K_2O BIOACTIVE GLASSES.

[1,2]Idris Y; [2]Ibrahim U, [2]Mundi A A, [2]Idris M. M. [3]Isa, M.S, [4]Papa, M I
[1]Department of Physics, Federal University of Technology, Owerri, Imo State, Nigeria.
[2].Departmetn of Physics, Nasarawa State University, Keffi, Nasarawa State, Nigeria
[3]Department of Physics, Yobe State university, Damaturu, Yobe State, Nigeria.
[4]Navy Simulation Center, Nigerian Defence Academy, Kaduna State, Nigeria.
Correspondence: y.idris74@yahoo.com

https://doi.org/10.48153/jrrs/2023/MEER6525

Article info
First Submission
21th June 2023

Revised
24th July 2023

Accepted
14th September 2023

ABSTRACT

Background: Tin(IV) oxide (SnO_2) has favorable photon shielding properties due to its high atomic number (Z), which enables effective attenuation of gamma rays and X-rays. When incorporated into bioactive glasses, SnO_2 dopants enhance the overall photon shielding performance of the composite material. The high Z of Sn (Z=50) assists in attenuating the photons through photoelectric effect, Compton scattering, and pair production mechanisms.

Objective: The research is to assess photon and neutron shielding competence of SnO_2-reinforced $22Na_2O$ –$15B_2O_3$ –$45P_2O_5$ – (18 – x) K_2O – $xSnO_2$ (NBPK) (x = 0, 2, 4, 6, 8, and 10 Mol%) bioactive glasses for better radiation shielding.

Methods: In this study, the melt quenching process is assumed in making the glass system $22Na_2O$ –$15B_2O_3$ –$45P_2O_5$ – (18 – x) K_2O – $xSnO_2$, x = 0, 2, 4, 6, 8 and 10 mol %) using $NH_4H_2PO_4$, H_3BO_4, Na_2CO_3, K_2CO_3 [12]. Computational approach was applied to estimate for each value of x. The nominal compositions of the prepared glasses were given as S1-S6 and was run in the WinXCOM software. The XCOM code is a database for calculating mass attenuation coefficients at different photon energies [11, 13].The obtained value from WinXCOM (S1-S6) were transported to excel for further calculations and thereby taken to the origin software for graph plotting.

Results: The result of the simulation shows that as energy changes, the Mass attenuation coefficient (MAC) values of all the glass samples change in a similar way. As a result, the MAC values tend to be in the order of S1 < S2 < S3 < S4 < S5 < S6 for the majority of the energy spectrum. S1-S6's LAC maximums were 0.08, 0.45, 0.59, 0.71, 0.80, and 0.92, respectively. The greatest HVT was acquired for all glass tests with values 65.56, 13.28, 11.18, 10.26, 9.81, and 9.16 cm for S1-S6 accordingly. .

Conclusion: The calculated radiation interaction parameters revealed that S6 outperformed the other five bioactive glasses in this study as a photon, proton, and neutron absorber. In general, photon shielding applications may benefit more from the studied bioactive glasses than conventional concrete.

Keywords: WinXCOM software, effective electron density, mass density, Mass attenuation coefficient (MAC), linear attenuation coefficient (LAC), Mean free path (MFP), Halve value thickness (HVT), and Effective atomic number (Zeff).

Introduction

Radiation poses the greatest threat to humans and the environment today. Due to the increasing use of radiation in a variety of fields, it is therefore necessary to find suitable alternative shielding materials. Presently, lead (Pb) and conventional concrete are regarded as ideal neutron shielding materials, but they are prohibitively expensive, toxic, and ineffective [1, 11]. Finding radiation shielding materials that are useful, inexpensive, non-toxic, and effective has been the subject to a lot of researchers up to this point. It has been suggested that numerous commercial glasses, concretes, rocks, and alloys glasses are competing for radiation shielding materials [2, 10]. Glasses are increasingly being used as protective materials in applications that utilize radiation to absorb incoming photons that may harm workers and patients surrounding the radioactive source. There are currently hundreds of applications for radiation in a variety of fields, including energy generation and medicine [3]. Despite the benefits of radiation, precautions must be taken when dealing with radioactive sources as high-energy photons can be extremely harmful to the human body [4, 5]. Depending on the application, a variety of materials are frequently utilized for this purpose. Concrete is typically used as the absorber to line the walls of X-ray rooms because of its practicality and effective attenuation of X-rays. Despite the fact that concrete is susceptible to cracking and loses its water content after prolonged radiation exposure, it is sometimes necessary to use other materials because of this. Low glass transition temperatures, high thermal expansion coefficients, and low optical dispersions are just a few of the desirable characteristics of these glasses. They are likewise incredible attenuators against a large number of frequencies, have a high dielectric consistent, and low phonon energy [8, 9]. This work will therefore assess photon and neutron competency of SnO_2-reinforced with $22Na_2O – 15B_2O_3 – 45P_2O_5 – (18 – x)\ K_2O – xSnO\ (x \leq 10$ Mol% $)$ bioactive glasses for better radiation shielding.

Materials and Methods:

In this study, the melt quenching process is assumed in making the glass system $22Na_2O – 15B_2O_3 – 45P_2O_5 – (18 – x)\ K_2O – xSnO_2$, x = 0, 2, 4, 6, 8 and 10 mol %) using $NH_4H_2PO_4$, H_3BO_4, Na_2CO_3, K_2CO_3 [12]. Computational approach was applied to estimate for each value of x. The nominal compositions of the prepared glasses were given as S1-S6 and was run in the winXCOM software. The XCOM code is a database for calculating mass attenuation coefficients at different photon energies [11, 13].The obtained value from winXCOM (S1-S6) were transported to excel for further calculations and thereby taken to the origin software for graph plotting.

Calculation of radiation interaction parameters

The absorption of photons within any medium, may be described by several parameters. According to the Beer–Lambert equation, the transmission (T_x) of photons may be macroscopically represented by:

$$T_x = e^{-ut} \qquad (1)$$

Where T_x is the ratio of transmitted and incident measurable quantity (x) of the photon. X could be dose (energy or number flux/fluence) [13]. The absorber thickness is represented by t while the parameters μ is referred to as the linear attenuation coefficient (LAC) of the absorber. Generally, LAC is a function of absorber thickness, photon energy, and the chemical nature of the medium. When LAC is divided by the density of the absorber it is called mass attenuation coefficient (MAC) defined as:

$$MAC = \frac{\mu}{\rho} = \mu_m \qquad (2)$$

With ρ the mass density of the absorbing medium. In contrast, LAC, MAC is dependent not only on thickness but also on the nature of the absorbing material and the energy of the photon.

The sum of all possible photon absorption cross - sections, photoelectric (PA), Compton scattering, and photon pair production in the absorber is referred to as MAC [6]. Comparing the relative photon absorption capacities of various media can be done with the help of MAC and LAC.

Many other parameters can be adopted to measure the photon absorbing capacity of a different photon interacting medium. These are: mean free path (MFP), half-value layer (HVT), and the effective atomic number (Z_{eff}). They are related to LAC or MAC according to equations 3 -5.

$$MFP = \frac{1}{\mu} \qquad (3)$$

$$HVT = \frac{ln2}{\mu} \qquad (4)$$

$$Z_{eff} = \frac{\sum_i WiAi\left(\frac{\mu}{\rho}\right)i}{\sum_j \frac{WjAj}{Zi}\left(\frac{\mu}{\rho}\right)j} \qquad (5)$$

Where, W_i, Z_i, and A_i is the mass proportion, atomic number, and atomic mass number of the $_i$th elemental component of the absorbing glass. The MAC values of S1-S6 glasses were evaluated through the use of WinXCOM computer code for photon energies between 0.1 MeV and 10 MeV. Equation 1-5 were used to calculate LAC, MFP, HVT, and Z_{eff} respectively [12].

.

Results:

The shielding competencies of $22Na_2O$ –$15B_2O_3$ – $45P_2O_5$ – (18 – x) K_2O – $xSnO_2$ metal oxide of different mixing ratio (x = 0, 2, 4, 6, 8, and 10 mol%) was investigated. The WinXCOM computer software was used to generate the mass attenuation coefficient for the energy range 0.10 to 10 MeV. The linear attenuation coefficient, halve value thickness, mean free path and effective atomic number were calculated for comparisons between the glasses S1, S2, S3, S4, S5 and S6 in search for good shielding materials. The chemical compositions and densities of the investigated glasses are summarized in Table 1 and the comparisons are shown in Figure 1, 2, 3, 4 and 5 respectively.

Table 1. Codes, Chemical compositions and Densities of the glasses

Glass mixture			Weight fraction				Density
Code	B	O	Na	P	K	Sn	
S1	0.05	0.44	0.16	0.20	0.15	0.00	2.31
S2	0.05	0.45	0.16	0.20	0.13	0.02	2.38
S3	0.05	0.45	0.16	0.20	0.12	0.03	2.42
S4	0.05	0.45	0.16	0.20	0.10	0.05	2.47
S5	0.05	0.45	0.16	0.20	0.08	0.06	2.51
S6	0.05	0.45	0.16	0.20	0.07	0.08	2.56

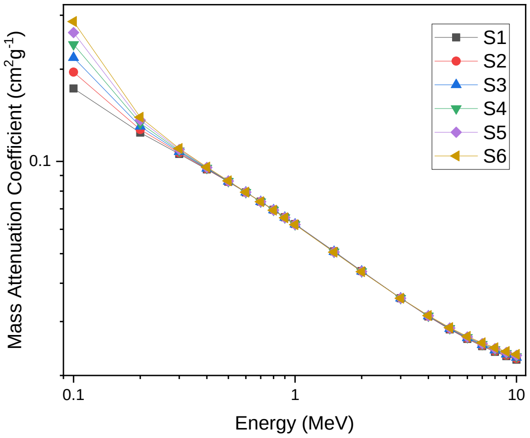

Figure 1. MAC values as a function of photon energy for NBPK-glasses

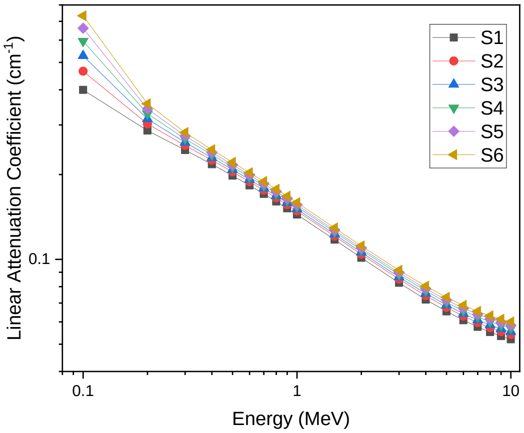

Figure 2. LAC values as a function of photon energy for NBPK-glasses.

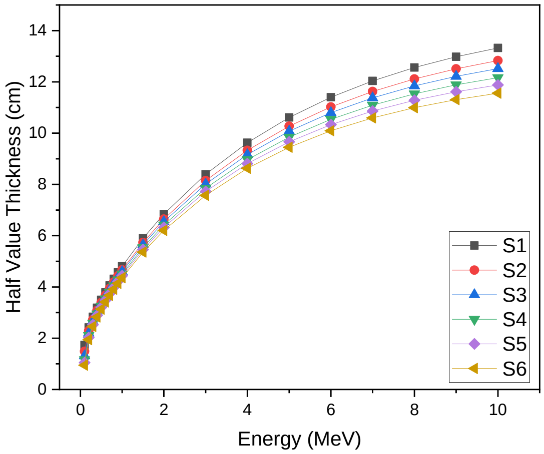

Figure 3. Half Value thickness values as a function of photon energy for NBPK-glasses.

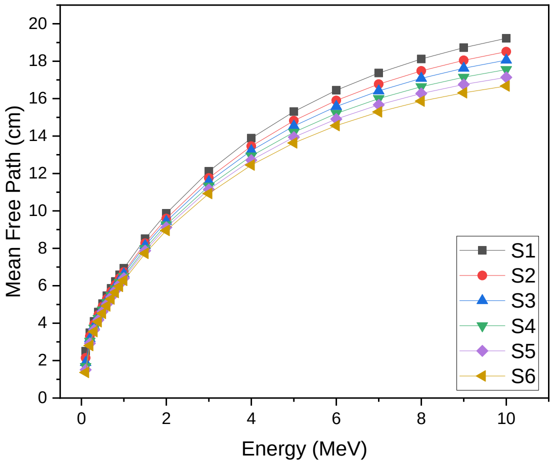

Figure 4. Mean free path values as a function of photon energy for NBPK-glasses.

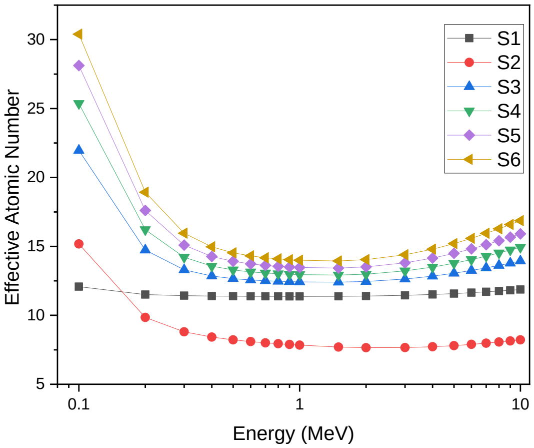

Figure 5. Effective Atomic Number (Z_{eff}) values as a function of photon energy for NBPK-glasses.

Discussion:

The study conducted by Rammah et al. [12] in 2021 on SrO-reinforced potassium, sodium, borophosphate, bioactive glasses is comprehensive and provides valuable insights into the properties and radiation attenuation competence of these materials. The optical absorption spectra and the calculated MAC, LAC, HVT, and MFP values provide essential information about the radiation attenuation capabilities of the glasses. The trend of decreasing MAC and LAC values with increasing SrO content indicates improved radiation absorption properties. This aligns with the authors' assertion that the studied bioactive glasses could perform better than ordinary concrete for photon shielding applications.

This study investigated the photon shielding capabilities of glass samples with different compositions, specifically varying amounts of sodium oxide (Na_2O), boron oxide (B_2O_3), phosphorus pentoxide (P_2O_5), potassium oxide (K_2O), and tin (IV) oxide (SnO_2). To assess the shielding efficiency, various parameters such as mass attenuation coefficient (MAC), linear attenuation coefficient (LAC), half value thickness (HVT), mean free path (MFP), and effective atomic number (Z_{eff}) were calculated across a range of photon energies (0.1 to 10.0 MeV).

Variation of MAC and LAC with Energy:

The MAC and LAC values for all glass samples follow similar patterns with changes in photon energy. The graphs (figure 1 & 2) show three distinct peaks at 0.8, 3.0, and 7.0 MeV, which can be attributed to the K-absorption edges of the Sn atoms in the SnO_2 component of the glass. The maximum (minimum) MAC values were 0.17 (0.02), 0.20 (0.02), 0.22 (0.02), 0.23 (0.02), 0.26 (0.02), and 0.29 (0.02) and The LAC maximum were 0.08, 0.45, 0.59, 0.71, 0.80, and 0.92 cm2/g for S1- S6 respectively. Based on the MAC and LAC values, it can be suggested that the increase in the SnO_2 content of the glass leads to increase in the effective electron density and mass density of the material thereby leading to better photon attenuation capacity [6].

The HVT values of all glass samples increase with an increase in photon energy but show a slight drop at the end (figure 3). The highest HVT values are obtained for S1 (lowest SnO_2 content) and decrease as the SnO_2 molar concentration increases in the glass matrix 65.56, 13.28, 11.18, 10.26, 9.81, and 9.16 cm for S1 - S6, respectively. This trend is consistent with the results of MAC and LAC and also consistent with the findings of Rammah et al [12]. The decrease in HVT with increase in SnO_2 corresponds to the increase in MAC and LAC values for all energies. Thus, the increase in SnO_2 improve the photon shielding parameter of HVT [2, 3, 5].

The trend of mean free path (MFP) with energy and glasses' content follow the same behavior as that of HVT (figure 4). Higher MFP implies that photons travel through longer distance before interacting, hence, higher HVT [7, 8, 10]. This means that more of such material's thickness is required to shield photon absorption to a certain level compare to one with lower HVT values [7, 8]. Generally, the MFP is lower at lower energy, increasing with energy and decreasing with increase in SnO_2 across the glass species. The maximum values of MFP were obtained with magnitudes of 12.31, 2.22, 1.69, 1.42, 1.25, and 1.08 cm respectively for S1-S6. The reduction in the magnitude of MFP as SnO_2 content of the glass increased is consistent with the results of MAC, LAC and HVT.

However, the measure of electron number present in a composite material is given in terms of the effective atomic number (Z_{eff}) [9, 10, 11]. The Z_{eff} of all the glass samples as function of photon energy is given in Figure 5, the Z_{eff} had overlaps each other at 0.16 MeV. These are due increase in the number of electrons available per mole for photon interactions. The increase in Z_{eff} is directly responsible for the lower MFP, HVT, and higher MAC values as Sn molar concentration increased in the glass samples. Generally, the photon shielding capacity of the glass was improved as the SnO_2 concentration was increased.

Overall, the results suggest that increasing the SnO2 content in the glass composition leads to enhanced photon shielding properties, making the glass more effective for attenuating photon interactions. The findings are essential in understanding the behavior of the glass samples at different photon energies and can be valuable for applications where effective photon shielding is required, such as in radiation shielding materials for medical and industrial purposes.

Conclusion

The study presents a comprehensive analysis of the photon shielding capabilities of glass samples with varying SnO_2 content. The findings provide valuable insights into the role of SnO_2 in enhancing the photon attenuation capacity of the glass and hold promising implications for the development of efficient radiation shielding materials. With further research and refinement, these glass composites have the potential to contribute significantly to advancements in radiation protection technologies across various sectors.

The density of the prepared glasses has been found to increase with an increase in the SnO_2 content, whereas an opposite trend has been observed in the molar volume.

Therefore, the results of the calculated radiation interaction parameters showed that S6 is a better photon, proton and neutron absorber compared to the other five bioactive glasses in this study. Generally, the studied bioactive glasses can function better than ordinary concrete for photon shielding applications.

Competing Interest

Authors have declare no competing interest exist.

References

1. Y.S. Rammah, M.S. Al-Buriahi, A.S. Abouhaswa. B2O3–BaCO3–Li2O3 glass system doped with Co3O4: structure, optical, and radiation shielding properties. Physics of Condense Matter. 2019; 576 411717.
2. Al-Buriahi, M. S., Sayyed, M. I., Al-Hadeethi, Y. Role of TeO2 in radiation shielding characteristics of calcium boro-tellurite glasses, Ceramic International journal. 2020; 46(1) 13622 -13629.
3. Sastry, S.S., Rupa, B., & Rao, B.R.V. Structural and optical properties of vanadium doped alkaline

earth lead zinc phosphate glasses. Indian J. Pure Appl. Phys. 2014; 52, 491–498.

4. Sayyed, M.I., Al-Hadeethi, Y., Al-Shammari, M., Ahmed, M., Al-Heniti, S.H., & Rammah, Y.S. Physical, optical, and gamma radiation shielding competence of newly borotellurite based glasses: TeO2–B2O3–ZnO–Li2O3–Bi2O3. Ceramic International. 2021; 47,611–618.

5. Sayyed, M.I., Almuqrin, A.H., Kurtulus, R., Javier-Hila, A.M.V., Kaky, K., & Kavas, T. X-ray shielding characteristics of P2O5–Nb2O5 glass doped with Bi2O3 by using EPICS2017 and Phy-X/PSD. Applied Phys. A. 2021; 127, 243.

6. Rammah YS, Olarinoye IO, El-Agawany FI, El Sayed Y, Ibrahim S, Ali AA. SrO reinforced potassium sodium borophosphate bioactive glasses: Compositional, physical, spectral, structural properties and photon attenuation competence, Journal of Noncrystalline solids. 2021;559:120667. Available:https://doi.org/10.1016/j.jnoncrys

7. Roman, J., Michał, A.G., Wojciech, K., & Mariusz, D. Application of a non-stationary method in the determination of the thermal properties of radiation shielding concrete with heavy and hydrous aggregate. Int. J. Heat Mass Transf. 2019; 130, 882–892.

8. Reza, B., Alireza, K.M., Seyed, P.S., Bakhtiar, A., & Mojtaba, S. Determination of gamma-ray shielding properties for silicate glasses containing Bi2O3, PbO, and BaO. J. Non-Cryst. Solids. 2018; 479, 62–71.

9. Halimah, M.K., Azuraida, A., Ishak, M., & Hasnimulyati, L. Influence of bismuth oxide on gamma radiation shielding properties of borotellurite glass. J. Non-Cryst. Solids. 2019; 512, 140–147.

10. El-Samrah, M.G., Abdel-Rahman, M.A., & El-Shazly, R.M. Effect of heating on physical, mechanical, and nuclear radiation shielding properties of modified concrete mixes. Radiation Phys. Chem. 2018; 153, 104–110.

11. Ashok, K. Gamma-ray shielding properties of PbO-Li2O-B2O3 glasses. Radiation Phys. Chem. 2017; 136, 50–53.

12. Y.S. Rammah, I.O. Olarinoye, F.I. El-Agawany, El Sayed Yousef, S. Ibrahim, A.A. Ali. SrO-reinforced potassium sodium borophosphate bioactive glasses: Compositional, physical, spectral, structural properties and photon attenuation competence. Journal of Non-crystalline solids 2021; 559, 120667.

13 Idris M. Mustapha, Atimga B. James and Sulayman M. Bello. Photon Shielding Characterization of SiO_2-PbO-CdO-TiO_2 Glasses for Radiotherapy Shielding Application. Asian Journal of Research and Reviews in Physics 2021; 4(4): 32-38.